

Stratification of the Fe/Si(001)2×1 interface by heat treatment of the wetting layer

© N.I. Plusnin

Military Orders of Zhukov and Lenin Red Banner Academy of Communications. Marshal of the Soviet Union S.M. Budyonny
Ministry of Defense of the Russian Federation, St. Petersburg, Russia
e-mail: plusnin@dvo.ru

Received July 26, 2022

Revised September 27, 2022

Accepted October 5, 2022

The study was carried out by LEED, AES, EELS and AFM methods. Films of Fe/Si(001)2×1 were obtained at substrate temperatures of 30°C and source temperatures of 1250°C. Wetting layer (WL) Fe on Si(001)2×1 was formed by two-stage annealing at temperatures and thicknesses of 500°C and 250°C and 1 monolayer (ML) and 3 ML, respectively. Analysis and interpretation of the data obtained, taking into account possible reaction patterns, showed that after annealing at 1 ML thickness, the Fe composition corresponded to 2 ML Si/Fe. Further, at 2 ML, it changed to Fe/Si/Fe, at 3 ML, it changed to Fe–FeSi, and after annealing, to FeSi. At 4 ML, there was formation of FeSi/FeSi₂ film. And, further, at 7 ML and 10 ML, the composition of the films became Fe₃Si/FeSi₂ and, respectively, Fe/Fe₃Si/FeSi₂. At the same time, the upper Fe₃Si layers were coated with 0.6 ML and the Fe layers with 0.3 ML of segregated Si atoms, which number increased, after annealing at 250°C, to 0.6 ML in the latter case. In the obtained Fe film, the size and average grain height were 10–20 nm and, respectively, ~ 0.4 nm.

Keywords: interface, wetting layer, multilayer film, layer composition, surface reaction patterns, Fe, Si(001)2×1.

DOI: 10.21883/TP.2023.01.55449.191-22

Introduction

Imperfection of the metal-silicon contact used in the nanoelectronics is related to the fact that the metal starts growing on silicon by being mixed with a substrate and by forming a silicide layer, which deteriorates transport characteristics of the contact. The matter is that as the contact is formed the hidden stress energy is accumulated and after some threshold this energy is spontaneously released as thermal energy, thereby increasing the diffusion and causing the reaction with mixing at the interface and forming non-volume and volume silicide phases.

One of the ways of improving the contact characteristics is to use interlayers of various two-dimensional (2D) materials (for example, MoS₂ and WS₂ [1]), which prevent formation of defects, alloys and chemical compounds at the interface. Nevertheless, it is important to obtain a stable and ultrafine metal-semiconductor contact without introducing any foreign materials. A promising method of obtaining such the contact could be its freezing by metal deposition at the reduced vapor temperature and the substrate's room temperature and subsequent moderate annealing (which does not cause disruption of the layer continuity) at the stage of formation of the wetting layer.

Recently, the contact freezing after two monolayers (2 ML) has discovered the growth of the „nanophase“ or nanocluster wetting (ν -WL in abbreviation) layer of the thickness of 2–4 ML [2]. And its formation agrees with a theory of nucleation and growth at the non-coherent interface [3] and is confirmed by experimental studies [4–7]. The detection of ν -WL makes it possible to re-look at the

physics of formation of the metal-semiconductor interface and is of high practical importance for manufacturing solid-state nanostructures in the electronics. Control of the substrate temperature (annealing) and the thermal power and geometry of the metal vapor stream makes it possible to change the thickness and composition of ν -WL [8], thereby affecting the structural condition of the metal film and its silicon contact.

The initial stages of Fe growth on the single-crystal silicon have been studied for a long time, but their results were not quite clear and sometimes contradictory [9–12]. In particular, based on the obtained data the work [9] has stated that the Fe growth on Si(001) was accompanied by mixing to be activated by the reaction at the interface of Si and Fe. But it did not take into account silicon segregation — release of its excessive insolubles on the film surface. Another example includes the study of the growth of Fe on Si as carried out in the work [11]. By a position of the maximum of the function of distribution of the radial atoms (1.9–2.0 Å) (as determined by a thin structure of the peak L₂₃–Fe (710 eV) of the electron loss spectrum), this work has concluded that at 3–4 ML Fe the silicide was formed. But this position did not correspond to the position of the maximum in the silicides as obtained by annealing the thicker film 70 Å [11], as for them the position of this maximum is within the range 2.3–2.6 Å.

We think that inaccuracy of interpretation of the results of these works and some other earlier works is related to the fact that it did not take into account formability of the segregated and wetting layers, which can have the non-volume atomic structure and density. Therefore,

the composition has been quantitatively analyzed without taking into account these layers. And the usage of the Auger analysis standard mode made it difficult to take it into account at the high energy of the beam. In addition, it did not take into account compatibility of the probing depth's Auger analysis with the other methods, like the electron energy loss spectroscopy (EELS) or the photoelectron spectroscopy. Negligence of these factors in the works [13–16] requires revision of the conclusions made therein. Moreover, these works did not take into account the influence of the temperature of the substrate and/or metal vapors and other deposition conditions (the geometry, the deposition rate, etc.). Although, it is known that the reduction of the substrate temperature from 300 to 100 K [17–20] and the reduction of the thermal power of the metal vapors [8] freeze the interface and shift all the growth stages into the area of the smaller thickness. All this has made it impossible to generalize the results of the studies of the various authors and the groups.

This is the reason why we have studied the growth of the Fe film on Si(001) in the identical conditions of the growth (in the same chamber, on the same holder, with the same source) at the identical and optimum conditions of the analysis at the probing depth 3 ML (the same for the Auger electron spectroscopy (AES) and EELS), with the minimum heat transfer of the vapor and taking into account the dependence on the substrate temperature.

Nevertheless, a role of the wetting and segregated layers in formation of the Fe/Si-substrate interface has not been previously studied. In addition, the density of the growing phases was not compared with the density of the volume phases of the same composition. The further studies [4–6], were required to demonstrate by means of EELS and the atomic-force microscopy (AFM) [5,6] that ν -WL is a loose structurally heterogeneous phase and has a nanocluster structure (the latter fact is confirmed by the data of the work [16]).

However, the role of the wetting and segregated layers in formation of the contact would become more apparent, if it is in a more equilibrium condition. For this purpose, the present work has the wetting layer Fe on Si(001) annealed to have formed the contact thereon. It has turned out that the bidimensionally-lamellar nature of the composition of this layer results in the formation of the FeSi₂ interlayer during the Fe growth thereon, and this interlayer contributes to formation of a quite stable stratified nanofilm Fe/Fe₃Si/FeSi coated by the segregated silicon.

1. Materials, methods and technique of the experiment

The experiment has been carried out in the ultrahigh-vacuum (UHV) chamber fitted with the electron spectrometer for AES and EELS spectrum analysis and the low energy electron diffraction analyzer (LEED) (both by RIBER). Fe has been deposited from a Fe strip source at a small distance

(~ 2 cm) to the two Si substrates. These substrates were assembled on a rotating holder being used to place them against the sources. The substrates were commercial silicon plane of the *n*-type Si(100) with the specific resistance $\rho = 4.5 \Omega \cdot \text{cm}$, which were cut into rectangular samples sized as $18.0 \times 5.0 \times 0.42$ mm. In order to obtain the atomically pure surface of the samples, they were chemically cleaned, assembled on the sample holder and loaded into the UHV chamber and cleaned by the high-temperature flash annealing at $T = 1200^\circ\text{C}$ in accordance with the procedure previously described in [8].

The Fe films were deposited by many short pulses at the substrate temperature of $\sim 25^\circ\text{C}$ by evaporating of the thicker Fe coating on the Ta-foil at 1250°C . In turn, this coating on the Ta-foil was obtained by evaporating a small iron bar placed in a W-wire spiral heated to 1550°C . The samples were annealed at $T = 500$ and 250°C for the iron film thicknesses $d_{\text{Fe}} = 1$ ML and, correspondingly, $d_{\text{Fe}} = 3$ ML, as well as at 250°C for $d_{\text{Fe}} = 10$. After deposition of each iron batch and after annealing, the AES and EELS spectra were recorded at the primary electron energy $E_p = 300$ eV. After unloading to air, the samples with the Fe (10 ML) films were studied by AFM.

The thickness of the Fe film was determined by the deposition rate. In doing so, the deposition rate was initially calibrated using a quartz microbalance. After this, the deposition rate was adjusted by the decay rate of the Si Auger peak from the substrate in dependence of the intensity of the Si Auger peak from the substrate on the Fe film thickness, using a recursive method of quantitative Auger analysis for this. The layer thickness determines a quantity of atoms therein and assumes that the atoms therein have the same surface density as in the substrate. This determination is usually used for very thin films and provided in two different units of measurement: 1) the nanometers (or angstroms) and 2) a number of the monolayers. The first case includes the volume occupied by the atoms divided by the area of the surface occupied by the atoms. The second case includes the number of the deposited atoms divided by the number of the atoms in one monolayer of the substrate for a given face of the substrate.

The second method used two factors. The first factor was that the increment of the thickness (Δd) of the Fe film and the time intervals were constant for each deposition due to stability of the rate of deposition from the source. The second factor was that the Auger signal at the initial growth stage weakly depended on a growth mode (mixing or the pseudo-lamellar growth). In order to ensure the second factor, the probing depth was set to be 3 ML.

First of all, the first points of the dependences of the AES peaks of Si and Fe on d (at the film thickness below 1 ML) Δd (the thickness difference for the adjacent points) was evaluated for the simplest two-layer model of the pseudo-lamellar growth (in the first approximation). Later, the real growth mechanism was determined in the second approximation (the dependences of the composition of the lamellar film on the thickness) and, thereafter,

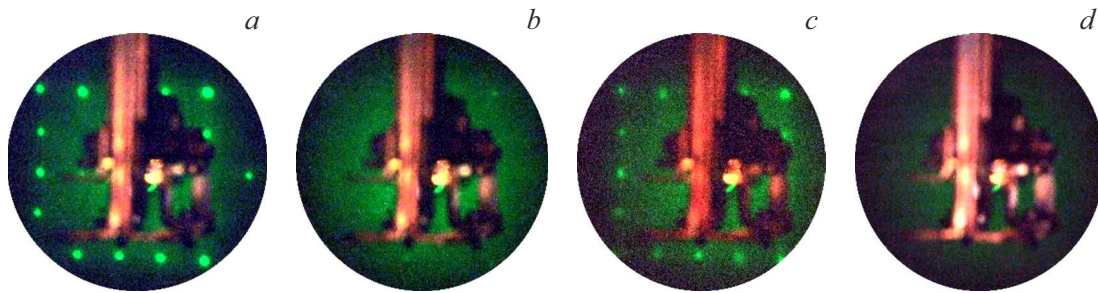


Figure 1. LEED-picture of the Fe films on Si(001)2×1 before (a) and after (b) deposition of 1 ML Fe, after annealing 1 ML Fe at $T = 500^{\circ}\text{C}$ (c), as well as after deposition of the Fe monolayer over ν -WL (d) (4 ML).

the value Δd was adjusted by the next points, but in the new model (in the second approximation) with a composition of the layers corresponding to the found growth mechanism. Finally, the total thickness was determined by multiplying Δd to the number of the steps Δd . In the second approximation, the composition and the thickness of the layers were determined in the three-layer model: „s-Si/Fe_xSi/Si-substrate“, where s-Si — the segregated Si. At the same time, for the Auger signals Fe and Si in the different layers the formulas were used, respectively: $(I/I^0)[1 - \exp(-d/L)]$ and $(I/I^0) \exp(-d/L)$ at $L = 3$ ML ($E_p = 300$ eV [4]), where L — the probing depth during the Auger analysis.

2. Results and discussion

After application of 1 ML Fe to Si (001)2×1 the LEED-picture of the clean surface (Fig. 1, a — the light-green reflections on the dark-green background (in the online version); the part of the picture is covered by the sample holder) was changed to the background with reflections — very weak in terms of the intensity (Fig. 1, b). And after annealing 1 ML Fe at 500°C , this background disappears and the LEED-picture is transformed into a structure Si(001)2×1-Fe less bright one as for the clean surface Si(001)2×1 (Fig. 1, c), which corresponds to 2 ML of the epitaxial Si on the two-dimensional layer of Fe as shown by the AES analysis (see below). With further deposition irrespectively of the annealing, the LEED-picture got a background without any reflections, which is similar to the one shown on Fig. 1, d for 4 ML. In all the cases, the background on the LEED pictures is indicative of the nanocrystalline structure of the film, in which the diameter of the nanocrystals does not exceed the length of the LEED coherency 10–20 nm (which is true at the energy 50–100 eV).

Fig. 2 shows the obtained spectra of AES and EELS, respectively, which are grouped in families in order to show the dependence of the spectra on the thickness of deposited iron (to the right of the spectra). Fig. 3, a shows the amplitudes of the Auger peaks $I_{\text{Fe}}(d)$ and $I_{\text{Si}}(d)$ in dependence on the thickness and the calculated curves (the

dotted lines) for the model of the pseudo-lamellar growth. Fig. 3, b shows the dependence of the thickness of the segregated Si on the thickness of Fe for the two models: s-Si/Fe/Si-substrate and s-Si/Fe₃Si/Si-substrate.

The calculated curves (dotted) of Fig. 3, a show the exponential change $I_{\text{Fe}}^0/I_{\text{Si}}^0 \exp(-d/L)$ of the Auger signal for the probing depth $L = 3$ ML and the experimentally found relationship $I_{\text{Fe}}^0/I_{\text{Si}}^0 = 0.75$ for the bulk samples Fe and Si. On Fig. 3, a breaks, surges and deviations of the solid AES-curves from the dotted curves show the following stages: (I) 0–1 ML Fe — the growth WL, (II) the annealing 1 ML Fe — the rearrangement WL, (III) 2 ML Fe — the growth WL, (IV) 3 ML Fe — the growth ν -WL, (V) the annealing 3 ML Fe — the rearrangement ν -WL, (VI) 4 ML Fe — the iron growth, (VII) 5–7 ML Fe — the growth of iron silicide, (VIII) 8–10 ML — the Fe growth and (IX) 10 ML (the annealing) — the agglomeration of the Fe film.

The growth stage (I)'s weak deviation of the points Si and Fe from the dotted curves (the curves were calculated in accordance with the equations of Section 1) is indicative (similar to the results of [14]) of the pseudo-lamellar growth WL Fe (in which, unlike the layer-by-layer growth, each subsequent layer starts after completion of the previous one due to the defects of the substrate surface and the non-equilibrium growth conditions).

The unequal deviation of the points in the dotted circle for Si and Fe after the annealing stage (II) is indicative of immersion of Fe under the Si layer: the immersion depth is evaluated to be 2 ML by the decay of the Auger peak Fe. The growth stage (III)'s proximity of the experimental points to the dotted curve again shows the pseudo-lamellar growth of Fe with formation of the three-layer film Fe(1 ML)/Si(2 ML)/Fe(1 ML).

The growth stage (IV)'s small and equal deviation of the experimental points from the dotted curve shows the mixing of the lower layers and formation of the lamellar Fe(1 ML)/FeSi(2 ML) film. After the annealing ν -WL at the stage (V) the equal deviation of the points from the dotted curve shows the formation of FeSi ν -WL of the thickness 3 ML.

In the stage (VI) during the growth the Fe stresses in the FeSi film relax with energy release, whereas the film

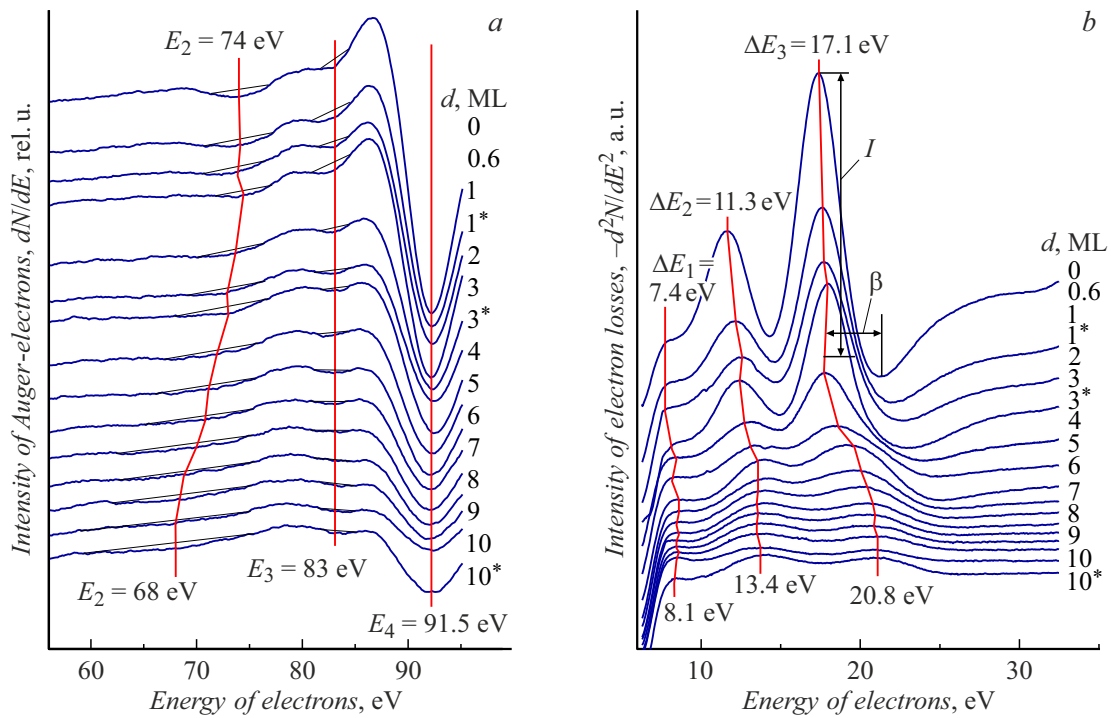


Figure 2. Spectra of AES- (a) and EELS-films (b) of Fe on Si(001)2×1. The lines — the guides for eyes which indicate the peak position: *a* — E_4 — the main Auger peak Si, and E_2 and E_3 — its plasmon and interband satellites in AES; *b* — E_1 — the peaks of the interband transitions, and ΔE_2 and ΔE_3 — the peaks of the surface and bulk plasmon losses in EELS, respectively.

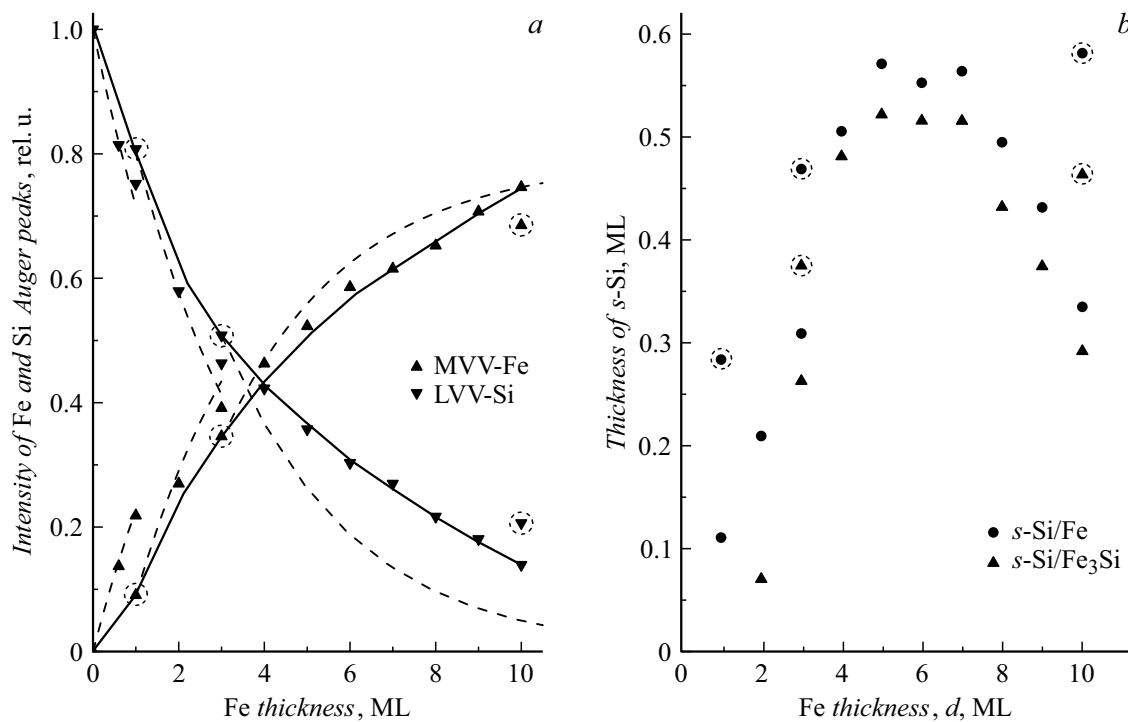


Figure 3. Dependences on the Fe thickness: *a* — the intensities of the Auger peaks of Si (▼) and Fe (▲), after deposition (the points) and annealing (the points in the dotted circles at 1, 3, 10 ML) of the Fe films on Si (001); *b* — the thicknesses of the segregated Si for the three-layer models: *s*-Si/Fe/Si-substrate and *s*-Si/Fe₃Si/Si-substrate (in the circles — after the annealing). The dotted lines — the model of the pseudo-lamellar growth and the solid lines — the experimental dependences.

is thickened and the near-boundary layer of the substrate becomes less compact, this silicon mixes with the film and the silicide is formed, which is followed by segregation of the excessive silicon unsolved in the silicide on the film surface. It results in formation and epitaxial crystallization of FeSi_2 in the lower layers (see the EELS data below). The segregation of silicon on the surface of the upper layer of the FeSi film is matched with bigger deviation of the point Si from the dotted curve at 4 ML in relation to the point Fe (Fig. 3, *a*). Finally, the $\text{FeSi}(1 \text{ ML})/\text{FeSi}_2(3 \text{ ML})$ lamellar film is formed in accordance with the diagram of the chemical reaction: $1\text{Fe} + 3\text{FeSi} + 4\text{Si} = 1\text{FeSi} + 3\text{FeSi}_2$, where „+4Si“ — silicon released from the substrate and input to the film during the mixing reaction.

Then, at the stage (VII) the $s\text{-Si}/(1-3) \text{ ML Fe}_3\text{Si}$ film is formed on top of 3 ML FeSi_2 . And the stage (VIII), 1–3 monolayers Fe grow on top of Fe_3Si . At the same time, the excessive portion Si coming from the substrate during its relaxation segregates on the film surface.

It is clear from Fig. 3, *b* that as Fe_3Si grows (the stage VII: 5–7 ML Fe), the thickness of the segregated Si remains almost unchanged, whereas it drops with increase of Fe. During the annealing, it increases both for the wetting layer and the Fe nanofilm.

It is obvious that the segregated silicon reduced the energy of the film-substrate system and plays a stabilizing role. The calculations (Fig. 3, *b*) have shown that when transferring from Fe_3Si (the stage VII) to Fe (the stage VIII) the thickness of $s\text{-Si}$ varies from 0.6 to 0.3 ML. The slight deviation of the points of Fig. 3, *a* after annealing 10 ML Fe (the stage IX) indicates the insignificant agglomeration of the Fe film. At the same time, as shown on Fig. 3, *b*, the amount of Si segregated thereon has increased from 0.3 to 0.6 ML.

Thus, prior to 1 ML Fe is chemically adsorbed and at 1 ML, 1 ML^(*), 2 ML, 3 ML and 3 ML^(*) (where ^(*) — means „after annealing“), the lamellar or homogeneous wetting layers grow, respectively: Fe; Si/Fe; Fe/Si/Fe; Fe/FeSi and FeSi. The deposition of the 1-st ML Fe to $\nu\text{-WL}$ of the FeSi composition results in excess of its stability threshold, $\nu\text{-WL}$ is collapsing and a new, more stable lamellar $\text{FeSi}/\text{FeSi}_2$ film is formed with the volume phase FeSi_2 . Later, the nanocrystals of the volume Fe_3Si and Fe are formed and grow on top of FeSi_2 , and these crystals are covered by the segregated Si atoms. The nanocrystals Fe_3Si and Fe form in accordance with the theory of the non-coherent interface with the large mismatch of the crystalline lattices [21], and Si segregates in accordance with the principle of minimization of free energy (see [22]).

The additional information about the growth mechanism can be obtained by the data on the growth position E_2 of the Auger peak (Fig. 2, *a*) and the energy difference $E_4 - E_2$ in the AES spectra in dependence on the thickness (Fig. 4). These differences show the increase of the electron and atomic density inside the surface layer within the depth 3 ML, which can contain the Si layer (beside the

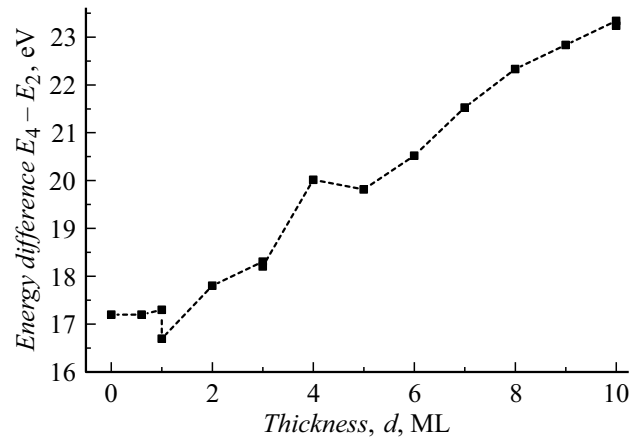


Figure 4. Dependence of the energy difference $E_4 - E_2$, which characterizes the concentration of the electron plasma in the interatomic bonds of the atoms Si, on the thickness.

film) adjoining the substrate and the layer of the segregated Si.

Up to 4 MLs, as it is clear from Fig. 2, *a* and 4, the value $E_4 - E_2$ is significantly less than the plasmon energy in the volume phases of the system Fe–Si (see below) and close to that for the Si substrate. It can be explained by formation (in the film) of the low-dimensional lamellar 2D WLs (1–2 ML) and the cluster $\nu\text{-WLs}$ (2–3 ML) with the reduced (due to adaptation of its structure to the substrate) density. These wetting layers are a two-dimensional lamellar or heterogeneous (over the surface) system, in which the Fe atoms adjoining the substrate are chemically bonded thereto. This bond causes tensile stresses by the film and compressive stresses by the substrate.

The tensile stresses increase the electron density of the adjoining area, while the compressive stresses increase it. Because of this and because of the thickness significantly lower than the wavelength of the plasmon oscillations in the film, the intensity of the plasmon losses from the film is significantly lower than from the bulk material. Hence, superposition of this small peak to the intensive peak by the substrate results in apparent proximity of the sum peak to the substrate peak. Nevertheless, the subtraction of this superposition from the sum peak (as done in the work [6]) still shows the lower electron density in the wetting layers.

It is clear from Fig. 4 that at the thickness of 1 ML and less there is no increase of the difference $E_4 - E_2$. Moreover, the annealing of 1 ML causes reduction of this difference, thereby indicating the reduction of the electron density in the two Si layers on top of the Fe layer. However, at $d = 2 \text{ ML}$, there is increase in the difference $E_4 - E_2$ to the value 17.8 eV.

If using the known formula for the volume energy of the plasmon $\Delta E = \hbar(4\pi n e^2)^{1/2} m^{-1/2}$ [23], then in the case of the volume silicon this change will provide its thickening $\sim 5\%$. At the same time, as in this case the film structure is $\text{Fe}(1 \text{ ML})/\text{Si}(2 \text{ ML})/\text{Fe}(1 \text{ ML})$, then there is

no bulk silicon in it (it is surrounded by the Fe monolayers) and the 2D Fe layers are pseudomorphic (they replicate the substrate structure). At the same time, the Fe atoms in the 2D layers ensure the same contribution of electrons to covalent bonds as in the bulk Si. Then, the evaluation $\sim 5\%$ may be referred to the lateral thickening of the entire 2D WL at 2 ML.

At the thickness 3 ML the stages of growth IV and annealing V form ν -WL Fe (1 ML) — FeSi(2 ML) and ν -WL FeSi (3 ML). But, as it is clear from Fig. 4, although the electron density in these layers increases, but it does not even come to the density of the most Si-enriched volume silicide — FeSi₂. At the same time, the annealing does not almost change this electron density, thereby showing that the main contribution to its value is by FeSi, but not 1 ML Fe on top.

At 4 ML (the stage of growth VI), the sharp increase of the difference $E_4 - E_2$ to 20.2 eV (the value corresponding to FeSi₂) (the values of the bulk plasmon losses for the volume see in [9–11]: 20.5 eV — FeSi₂; 21.1 eV — FeSi; 21.8 eV — Fe₃Si; 22.5 eV — Fe) indicates formation of the volume phase of the FeSi₂ composition in the film as predicted by the AES data. Although, as a whole, the lamellar film FeSi(1 ML) is formed — FeSi₂ (3 ML).

The further growth of the difference $E_4 - E_2$ corresponds to the growth at the stages VII–IX of the structures Fe₃Si(1–3 ML)/FeSi₂(4 ML) and, correspondingly, Fe(1–3 ML)/Fe₃Si(3 ML)/FeSi₂(4 ML). Note that at the thickness 5 ML the difference $E_4 - E_2$ even drops a little. It can be explained by further mixing of the FeSi(1 ML)/FeSi₂(3 ML) film and formation of the FeSi₂ (4 ML) layer under the Fe₃Si upper layer.

However, in EELS (Fig. 2, *b* and 5, *a*), at the stages of formation of Fe₃Si/FeSi₂ (VII) and Fe/Fe₃Si/FeSi₂ (VIII), there is no formation of the peaks of the surface (ΔE_2) and bulk (ΔE_3) plasmon losses of Fe₃Si and Fe, although the peak of the interband losses ΔE_1 reaches the respective value for these phases. Instead of it, the peaks FeSi₂ remain, and they weakly change their energy position with increase of the thickness. This peak behavior can not be explained by the segregated Si, as its thickness is less than the monolayer.

The contribution of the lower layer FeSi₂ after the stage VII is also excluded, as this layer is deeper than the probing area. In addition, taking into account the data of Fig. 4, it is hardly possible to adapt the density of Fe₃Si and Fe to the less dense silicon substrate (or the FeSi₂ interlayer) (due to their dense bulk stacking). Most likely, no contribution to these peaks by the Fe₃Si and Fe layers in EELS is due to the higher primary electron energy (300 eV) in comparison with the energy L₂₃VV of the Auger peak Si (92 eV) and to other geometry of excitation of the plasmon losses. Therefore, the EELS is mainly contributed by the underlying layer of the FeSi₂ composition and/or the upper segregated layer of Si.

Possible explanation of the reasons of no contribution by Fe–Si and Fe is also provided by consideration of amplitudes of the plasmon losses peaks (Fig. 2, *a*, 5, *b*). In

the EELS spectra, the amplitudes I_2 and I_3 of the losses peaks ΔE_2 and ΔE_3 , to the thickness of 2 ML, with increase of the thickness, decrease faster than for the substrate peak (I_2^* and I_3^*) at the theoretical pseudo-lamellar growth (the dotted curves of Fig. 5, *b*). But with the bigger thickness, it decreases for I_2 and I_3 differently: I_2 at 3 ML and after annealing 3 ML Fe stops decreasing and exceeds the theoretical value I_2^* , while I_3 continues smoothly decreasing with approaching the theoretical value only at 10 ML. In doing so, the difference $I_3^* - I_3$, as it is clear from Fig. 5, *c*, reaches the maximum at the thickness of 2 ML.

As mention above, the structure of the film at the thickness of 2 ML: Fe(1 ML)/Si(2 ML)/Fe(1 ML). Therefore, the contribution by these two-dimensional layers to the intensities I_2 and I_3 seems to be very small. It results in reduction of the intensity of the peaks. In addition, the intensity I_3 is additionally reduced due to formation of the „foreign (in terms of the density)“ layer of the high-pressure Si phase on the surface of the Si substrate. This layer can be formed as it is indicated by the data of [7] for optical reflection. After annealing of the Fe films, at the thicknesses of 1, 3 and 10 ML the behavior of the characteristic $I^*(d) - I(d)$ corresponds to „surfacing off“ 2 ML Si, mixing and agglomeration of the film.

The trend of slowdown of the I_3 fall and even of increase of I_2 after 4 ML Fe (Fig. 5, *b*) is obviously related to formation, at 4 ML, of the epitaxial FeSi₂ interlayer, which results in amplification of the agglomeration of the Fe₃Si and Fe layers growing thereon and which consequently determines the contribution to the intensity and energy of the EELS peaks. The transition from the two-dimensional lamellar film to the nanophase one and then to the FeSi₂ interlayer confirms the behavior of the halfwidth of the peak of the bulk plasma losses (β_3) after 2, 3 and 4 ML as well (Fig. 5, *d*).

Thus, the bidimensionally-lamellar and nanophase structures of the film as well as the agglomeration of the film do not provide conditions required for collective excitation of the plasmon across the entire volume of the film, and the structural-phase rearrangement of the near-surface region of the substrate (formation of the „foreign“ (in terms of the density) layer) results in additional decay of the losses from the substrate. It reduced the contribution of the peaks of the losses by the film and the substrate to the EELS spectrum. Whereas, vice versa, formation of the epitaxial FeSi₂ interlayer results in increase of its contribution to the spectrum. As a result, after formation of the FeSi₂ interlayer at 4 ML the spectra mainly exhibit only the peak from FeSi₂.

It is obvious that after FeSi₂ the Fe₃Si and Fe layers are formed to have a granular nanocrystalline structure. These layers and the silicon substrate are resiliently adapted to each other via the FeSi₂ layer. At the same time, the silicon substrate forms new defects of stacking and dislocation as caused by mismatch of the FeSi₂ and Si lattices. It is neither excluded that Fe₃Si and Fe are in a condition similar to the condition of the wetting layer.

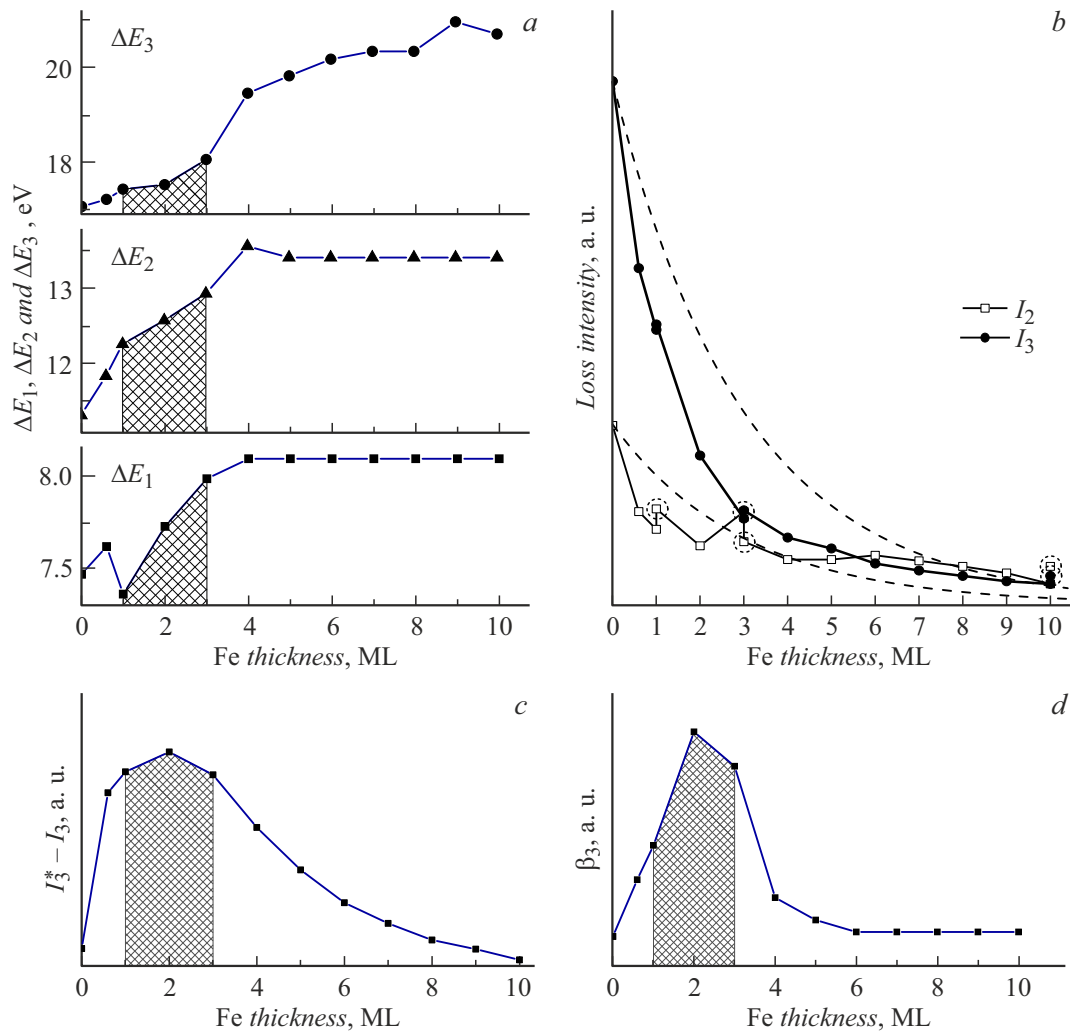


Figure 5. Dependences of the main parameters of the plasmon losses peaks on the thickness of the Fe film (before annealing, except for (b)): a — the peak energies $\Delta E_1, \Delta E_2$ and ΔE_3 ; b — the intensities of the losses peaks ΔE_2 and ΔE_3 (the dotted circle shows the points after annealing); c — the difference ($I_3^* - I_3$) between the theoretical (I_3^*) (for the substrate peak) and experimental (I_3) amplitudes of the peak ΔE_3 ; d — the width (β_3) of the peak ΔE_3 . The dashed region corresponds to the range of thicknesses, at which WL (1–3 ML) is formed.

Fig. 6 shows the AFM images (which were obtained in the semi-contact mode) of the Fe film of the thickness of 10 ML after its annealing at 250°C: before Fourier-filtration of the micro-relief (Fig. 6, a) and after this filtration (Fig. 6, b). In addition, it also shows the picture (Fig. 6, c) obtained by inverting the image in the „viscosity“ mode (where „viscosity“ corresponds to the phase shift of the AFM modulation signal). The obtained images (Fig. 6, a, c) reflect the topography of the sample surface, and Fig. 6, b, d reflects its morphology for „viscosity“ related to the density.

In the micrometre scale (Fig. 6, a, b), the film looks as solid and smooth, although it is intersected by the steps (the relief of the height below 1 nm is due to the steps). After the Fourier-filtration of the relief to remove the steps and height scaling (Fig. 6, c, d) it looks like a film with grains, which have the lateral sizes 10–20 nm and the average height of the relief ~ 0.4 nm.

The film morphology (the phase contrast mode) of Fig. 6, d replicates its topography to show the composition difference from the average one at the grain vertices. It corresponds to the vertex growth of pure iron. Although, it is obvious that the vertices have more „viscous“ layers therebetween, which contain silicon in a different degree (FeSi_2 , $s\text{-Si/Fe}_3\text{Si}$ and $s\text{-Si/Fe}$). Apparently, the surface-segregated layer of silicon atoms partially smoothens „the viscosity“ of the film.

The characteristics of the various stages of growth of the Fe film on Si(001) are tabularized.

As it is clear from the table, the similarity of the characteristics makes it possible to distinguish the above-listed stages of growth: 0–1 ML; 2–3 ML; 4 ML; 5–7 ML and 8–10 ML.

It is also clear that discrepancy of „the apparent“ composition as per the data of the AES satellite with the

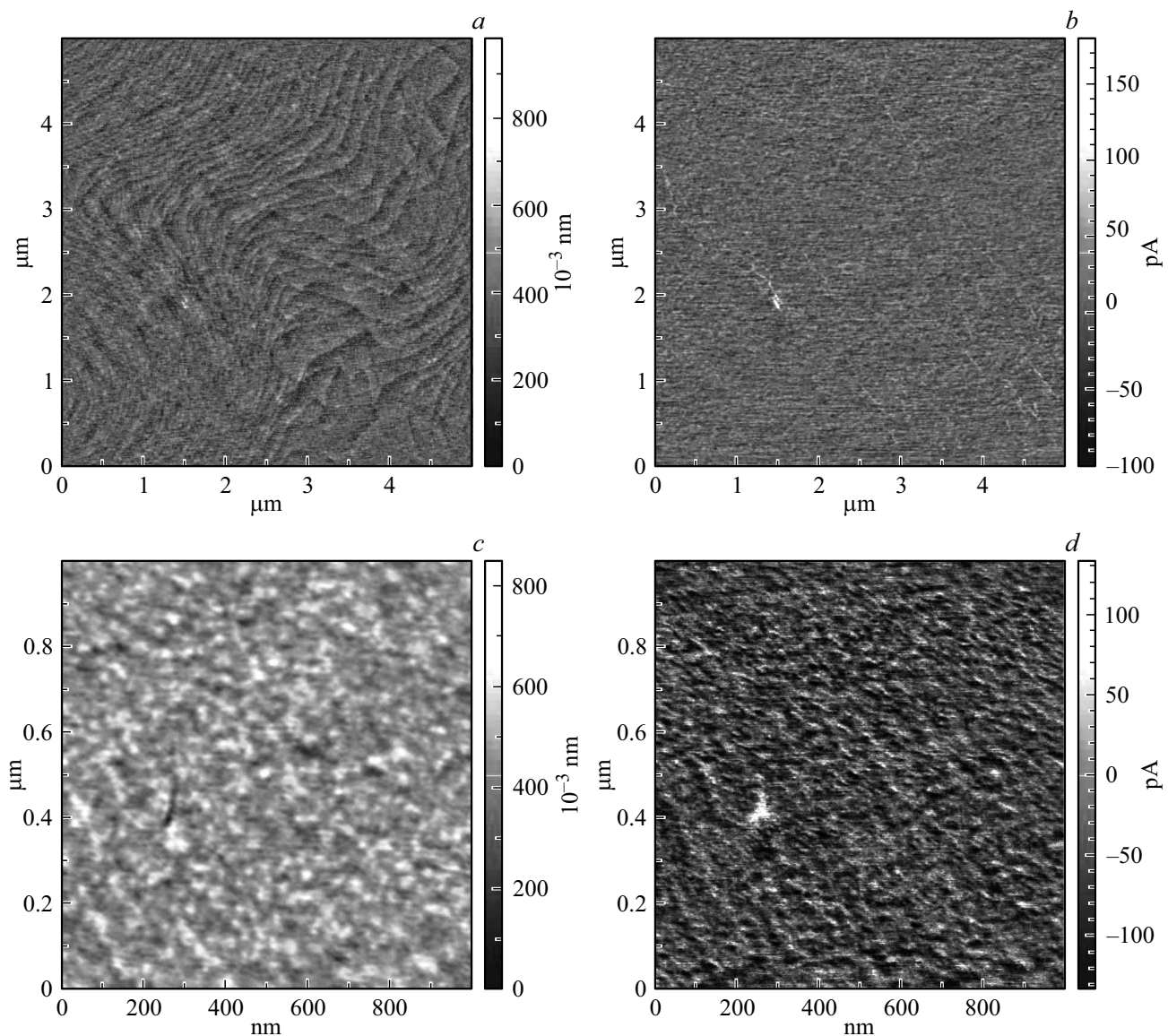


Figure 6. AFM-images of the relief (a), (c) and inverse „viscosity“ (b), (d) (the inversions of the image in the phase contrast mode) for the nanofilms Fe (10 ML) on Si(001): a, b — 5 × 5, c, d — 1 × 1 μm; a — after plane adjustment; c — after Fourier-filtration of the step relief.

composition determined based on EELS increases with the thickness. In general, this behavior reflects the transition from the wetting layer to the composition-stratified contact. At the thickness of 4–10 ML, the lamellar film forms from the silicide phases and iron. At these thicknesses, in the EELS case the plasmon losses are formed mainly by contribution of the substrate or the FeSi₂ layer adjoining thereto, so do the Fe₃Si and Fe layer in the AES-satellite case. For AES it is explained by the smaller energy of electrons (92 eV) experiencing the losses and the radial diagram of excitation of the plasmon oscillations, where an electron source is Si atoms (both the factors increase the sensitivity to the upper layers).

The formation of the epitaxial FeSi₂ layer obviously results in the delay (by 4–5 ML) of formation of magnetic

ordering as it is observed in [17]. However, in our case it is most likely that the magnetic ordering will be higher due to higher crystallinity of the Fe₃Si and Fe layers.

Summing up, the following model of the growth of the Fe film on Si(001) can be presented. Just after the stage of the chemical adsorption („adatoms“), first of all the 2D wetting coating is formed with one monolayer. It consists of the Fe monolayer covered with the two Si monolayers. Then, at the three monolayers a loose nanophase layer of the FeSi composition is formed. After this critical thickness, FeSi passes into the stable epitaxial phase of the FeSi₂F composition, on which the nanocrystals of the Fe₃Si volume phase grow, and, in turn, the Fe nanocrystals grow on them.

Each time, these transitions are accompanied by thickening of the phases with changing their composition

Stages of growth and characteristic of the films, as detected by the various methods

№	Phase type	d , ML, *(T_{Ann} , °C)	Structure as per LEED LEED (AFM)	Elementary composition AES (3-layer model)	Phase composition as per data	
					EELS (plasmon peak)	AES (plasmon satellite)
1	Adatoms	< 1	$2 \times 1 \downarrow$	Fe/Si(001)	~Si	~Si
2	2D-WL	1	$2 \times 1 \downarrow$	Fe/Si(001)	~Si	~Si
3	2D-WL	1 *(500)	$2 \times 1 \uparrow$	2-ML Si/Fe	~Si	~Si
4	2D-WL	2	Nanocrystals	Fe–Si/Fe	FeSi ₂ /Si	FeSi ₂ /Si
5	ν -WL	3	Nanocrystals	Fe/FeSi	FeSi ₂ /Si	FeSi ₂ /Si
6	ν -WL	3 *(250)	Nanocrystals	FeSi	FeSi ₂ /Si	FeSi ₂ /Si
7	Volume	4	Nanocrystals	FeSi/FeSi ₂	FeSi ₂ /Si	FeSi ₂
8	Volume	5–7	Nanocrystals	Fe ₃ Si/FeSi ₂	FeSi ₂ /Si	Fe ₃ Si
9	Volume	8–10	Nanocrystals	Fe/Fe ₃ Si/FeSi ₂	FeSi ₂	Fe
10	Volume	10 *(250)	(Grain size 10–20 nm)	Fe/Fe ₃ Si/FeSi ₂	FeSi ₂	Fe

and releasing of excessive silicon on the film surface. In addition, they are accompanied by relaxation of the stresses, clusterization or agglomeration of the films and nano-structuring of the boundary level of the substrate. The layers of the iron film adapt to the silicon substrate both due to ordering and segregation of excessive silicon on the film surface, which gradually dissolves in the film as the Fe thickness increases therein.

The evolution of the topography of the Fe nanofilm during the growth and after annealing at 250°C confirms this model [5,6]: at 1–2 ML the two-dimensional atomically-smooth film is formed, so is the nanogranular film at 3–7.5 ML, and at 7.5–15 ML the Fe nanofilm is formed and covered by crests (supposedly, of the segregated Si layer) with a relief height within the range 1–1.5 nm. It is obvious that no crest in the film obtained on the annealed wetting layer is indicative of its higher stability. Note that at this the grain size and the relief height of the Fe film do not exceed those for the film obtained in the work [16] without annealing the wetting layer. It means that the annealing of the wetting layer did not deteriorate the film structure, but provided its higher stability (at least to 250°C) as well.

Conclusion

The work has found the transition from the two-dimensional lamellar to two-dimensional nanophase-cluster structure of the wetting layer with the growth of the Fe wetting layer on Si(001)1×2, as obtained by the two-stage annealing. It has demonstrated the influence of the obtained wetting layer on the subsequent growth of Fe, which is manifested by formation of the FeSi₂ interlayer therefrom

and subsequent growth (on Si(001)) of the stratified film of the Fe/Fe₃Si/FeSi₂ composition with the Si layer segregated thereon. The results obtained can be used for developing the solid-phase method of the epitaxy of the ultrathin FeSi₂, Fe₃Si and Fe films on the surface of the single-crystal silicon.

Conflict of interest

The author declares that he has no conflict of interest.

References

- [1] S.-G. Nam, Y. Cho, M.-H. Lee, K.W. Shin, C. Kim, K. Yang, M.Jeong, H.-J. Shin, S. Park. *2D Materials*, **5** (4), 041004 (2018).
- [2] N.I. Plyusnin. *Tech. Phys. Lett.*, **44** (21), 64 (2018).
- [3] S.A. Kukushkin, A.V. Osipov. *Usp. Fiz. Nauk*, **168** (10), 1083 (1998). DOI: 10.3367/ufnr.0168.199810b.1083
- [4] N.I. Plyusnin. *News of Higher Educational Institutions. Mater. Electron. Technol.*, **20** (4), 239 (2017).
- [5] N.I. Plusnin, V.M. Il'yashchenko, S.A. Kitan', S.V. Krylov. *J. Phys.: Conf. Series. IOP Publishing*, **100** (5), 052094 (2008). DOI: 10.1088/1742-6596/100/5/052094
- [6] N.I. Plyusnin, V.M. Il'yashchenko, S.A. Kitan', S.V. Krylov. *Poverkhnost'. Rentgenovskie, sinkhrotronnye i neitronnye issledovaniya*, **9**, 86 (2009) (in Russian).
- [7] A.M. Maslov, N.I. Plusnin. *Defect and Diffusion Forum* (Trans Tech. Publications Ltd, 2018), v. 386. p. 15–20.
- [8] N.I. Plusnin, A.P. Milenin, B.M. Iliyashenko, V.G. Lifshits. *Phys. Low-Dimensional Structures (PLDS)*, **9–10**, 129 (2002).
- [9] J.M. Gallego, R. Miranda. *J. Appl. Phys.*, **69** (3), 1377 (1991). DOI: 10.1063/1.347276
- [10] Qi-Gao Zhu, Hiroshi Iwasaki, E.D. Williams, R.L. Park. *J. Appl. Phys.*, **60** (7), 2629 (1986).

- [11] X. Wallart, H.S. Zeng, J.P. Nys, G. Delmai. *Appl. Surf. Sci.*, **56** (58), 427 (1992). DOI: 10.1016/0169-4332(92)90265-Y
- [12] Y. Ufuktepe, M. Onellion. *Solid State Commun.*, **76** (2), 1919 (1990). DOI: 10.1016/0038-1098(90)90540-R
- [13] N.G. Gheorghe, M.A. Husanu, G.A. Lungu, R.M. Costescu, D. Macovei, C.M. Teodorescu. *J. Mater. Sci.*, **47** (4), 1614 (2012). DOI: 10.1007/s10853-011-5963-0
- [14] M. Fanciulli, S. Degroote, G. Weyer, G. Langouche. *Surf. Sci.*, **377**, 529 (1997). DOI: 10.1016/S0039-6028(96)01429-X
- [15] F. Sirotti, M. DeSantis, X. Jin, G. Rossi. *Appl. Surf. Sci.*, **65**, 800 (1993). DOI: 10.1016/0169-4332(93)90759-5
- [16] J. Alvarez, A.L. Vázquez de Parga, J.J. Hinarejos, J. de la Figuera, E.G. Michel, C. Ocal, R. Miranda. *Phys. Rev. B*, **47** (23), 16048 (1993). DOI: 10.1103/PhysRevB.47.16048.
- [17] F. Zavaliche, W. Wulfhekkel, H. Xu, J. Kirschner. *J. Appl. Phys.*, **88** (9), 5289 (2000). DOI: 10.1063/1.1314311
- [18] Z.H. Nazir, C.K. Lo, M. Hardiman. *J. Magn. Magn. Mater.*, **156** (1–3), 435 (1996). DOI: 10.1016/0304-8853(95)00930-2
- [19] W.-T. Tu, C.-H. Wang, Y.-Y. Huang, W.-C. Lin. *J. Appl. Phys.*, **109** (2), 023908 (2011). DOI: 10.1063/1.3537832
- [20] K. Rührschopf, D. Borgmann, G. Wedler. *Thin Solid Films*, **280** (1–2), 171 (1996). DOI: 10.1016/0040-6090(95)08248-4
- [21] D. Robertson, G.M. Pound. *Critical Rev. Solid State Mater. Sci.*, **4** (1–4), 163 (1973). DOI: 10.1080/10408437308245824
- [22] H. Wu, P. Kratzer, M. Scheffler. *Phys. Rev. B*, **72** (14), 144425 (2005). DOI: 10.1103/PhysRevB.72.144425
- [23] D. Pines. *Rev. Modern Phys.*, **28** (3), 184 (1956). DOI: 10.1103/RevModPhys.28.184